Evidence for an oscillatory signature in atmospheric neutrino oscillation

Y.Ashie,[1] J.Hosaka,[1] K.Ishihara,[1] Y.Itow,[1] J.Kameda,[1] Y.Koshio,[1] A.Minamino,[1] C.Mitsuda,[1] M.Miura,[1] S.Moriyama,[1] M.Nakahata,[1] T.Namba,[1] R.Nambu,[1] Y.Obayashi,[1] M.Shiozawa,[1] Y.Suzuki,[1] Y.Takeuchi,[1] K.Taki,[1] S.Yamada,[1] M.Ishitsuka,[2] T.Kajita,[2] K.Kaneyuki,[2] S.Nakayama,[2] A.Okada,[2] K.Okumura,[2] T.Ooyabu,[2] C.Saji,[2] Y.Takenaga,[2] S.Desai,[3] E.Kearns,[3] S.Likhoded,[3] J.L.Stone,[3] L.R.Sulak,[3] C.W.Walter,[3] W.Wang,[3] M.Goldhaber,[4] D.Casper,[5] J.P.Cravens,[5] W.Gajewski,[5] W.R.Kropp,[5] D.W.Liu,[5] S.Mine,[5] M.B.Smy,[5] H.W.Sobel,[5] C.W.Sterner,[5] M.R.Vagins,[5] K.S.Ganezer,[6] J.Hill,[6] W.E.Keig,[6] J.S.Jang,[7] J.Y.Kim,[7] I.T.Lim,[7] R.W.Ellsworth,[8] S.Tasaka,[9] G.Guillian,[10] A.Kibayashi,[10] J.G.Learned,[10] S.Matsuno,[10] D.Takemori,[10] M.D.Messier,[11] Y.Hayato,[12] A.K.Ichikawa,[12] T.Ishida,[12] T.Ishii,[12] T.Iwashita,[12] T.Kobayashi,[12] T.Maruyama,[12,*] K.Nakamura,[12] K.Nitta,[12] Y.Oyama,[12] M.Sakuda,[12] Y.Totsuka,[12] A.T.Suzuki,[13] M.Hasegawa,[14] K.Hayashi,[14] T.Inagaki,[14] I.Kato,[14] H.Maesaka,[14] T.Morita,[14] T.Nakaya,[14] K.Nishikawa,[14] T.Sasaki,[14] S.Ueda,[14] S.Yamamoto,[14] T.J.Haines,[15,5] S.Dazeley,[16] S.Hatakeyama,[16] R.Svoboda,[16] E.Blaufuss,[17] J.A.Goodman,[17] G.W.Sullivan,[17] D.Turcan,[17] K.Scholberg,[18] A.Habig,[19] Y.Fukuda,[20] C.K.Jung,[21] T.Kato,[21] K.Kobayashi,[21] M.Malek,[21] C.Mauger,[21] C.McGrew,[21] A.Sarrat,[21] E.Sharkey,[21] C.Yanagisawa,[21] T.Toshito,[22] K.Miyano,[23] N.Tamura,[23] J.Ishii,[24] Y.Kuno,[24] Y.Nagashima,[24] M.Takita,[24] M.Yoshida,[24] S.B.Kim,[25] J.Yoo,[25] H.Okazawa,[26] T.Ishizuka,[27] Y.Choi,[28] H.K.Seo,[28] Y.Gando,[29] T.Hasegawa,[29] K.Inoue,[29] J.Shirai,[29] A.Suzuki,[29] M.Koshiba,[30] Y.Nakajima,[31] K.Nishijima,[31] T.Harada,[32] H.Ishino,[32] R.Nishimura,[32] Y.Watanabe,[32] D.Kielczewska,[33,5] J.Zalipska,[33] H.G.Berns,[34] R.Gran,[34] K.K.Shiraishi,[34] A.Stachyra,[34] K.Washburn,[34] and R.J.Wilkes[34]

(The Super-Kamiokande Collaboration)

[1] *Kamioka Observatory, Institute for Cosmic Ray Research, University of Tokyo, Kamioka, Gifu, 506-1205, Japan*
[2] *Research Center for Cosmic Neutrinos, Institute for Cosmic Ray Research, University of Tokyo, Kashiwa, Chiba 277-8582, Japan*
[3] *Department of Physics, Boston University, Boston, MA 02215, USA*
[4] *Physics Department, Brookhaven National Laboratory, Upton, NY 11973, USA*
[5] *Department of Physics and Astronomy, University of California, Irvine, Irvine, CA 92697-4575, USA*
[6] *Department of Physics, California State University, Dominguez Hills, Carson, CA 90747, USA*
[7] *Department of Physics, Chonnam National University, Kwangju 500-757, Korea*
[8] *Department of Physics, George Mason University, Fairfax, VA 22030, USA*
[9] *Department of Physics, Gifu University, Gifu, Gifu 501-1193, Japan*
[10] *Department of Physics and Astronomy, University of Hawaii, Honolulu, HI 96822, USA*
[11] *Department of Physics, Indiana University, Bloomington, IN 47405-7105, USA*
[12] *High Energy Accelerator Research Organization (KEK), Tsukuba, Ibaraki 305-0801, Japan*
[13] *Department of Physics, Kobe University, Kobe, Hyogo 657-8501, Japan*
[14] *Department of Physics, Kyoto University, Kyoto 606-8502, Japan*
[15] *Physics Division, P-23, Los Alamos National Laboratory, Los Alamos, NM 87544, USA*
[16] *Department of Physics and Astronomy, Louisiana State University, Baton Rouge, LA 70803, USA*
[17] *Department of Physics, University of Maryland, College Park, MD 20742, USA*
[18] *Department of Physics, Massachusetts Institute of Technology, Cambridge, MA 02139, USA*
[19] *Department of Physics, University of Minnesota, Duluth, MN 55812-2496, USA*
[20] *Department of Physics, Miyagi University of Education, Sendai,Miyagi 980-0845, Japan*
[21] *Department of Physics and Astronomy, State University of New York, Stony Brook, NY 11794-3800, USA*
[22] *Department of Physics, Nagoya University, Nagoya, Aichi 464-8602, Japan*
[23] *Department of Physics, Niigata University, Niigata, Niigata 950-2181, Japan*
[24] *Department of Physics, Osaka University, Toyonaka, Osaka 560-0043, Japan*
[25] *Department of Physics, Seoul National University, Seoul 151-742, Korea*
[26] *International and Cultural Studies, Shizuoka Seika College, Yaizu, Shizuoka 425-8611, Japan*
[27] *Department of Systems Engineering, Shizuoka University, Hamamatsu, Shizuoka 432-8561, Japan*
[28] *Department of Physics, Sungkyunkwan University, Suwon 440-746, Korea*
[29] *Research Center for Neutrino Science, Tohoku University, Sendai, Miyagi 980-8578, Japan*
[30] *University of Tokyo, Tokyo 113-0033, Japan*
[31] *Department of Physics, Tokai University, Hiratsuka, Kanagawa 259-1292, Japan*
[32] *Department of Physics, Tokyo Institute for Technology, Meguro, Tokyo 152-8551, Japan*
[33] *Institute of Experimental Physics, Warsaw University, 00-681 Warsaw, Poland*
[34] *Department of Physics, University of Washington, Seattle, WA 98195-1560, USA*

(Dated: June 24, 2004)

Muon neutrino disappearance probability as a function of neutrino flight length L over neutrino energy E was studied. A dip in the L/E distribution was observed in the data, as predicted from

the sinusoidal flavor transition probability of neutrino oscillation. The observed L/E distribution constrained $\nu_\mu \leftrightarrow \nu_\tau$ neutrino oscillation parameters; $1.9 \times 10^{-3} < \Delta m^2 < 3.0 \times 10^{-3}\mathrm{eV}^2$ and $\sin^2 2\theta > 0.90$ at 90% confidence level.

PACS numbers: 14.60.Pq, 96.40.Tv

Recent neutrino experiments using atmospheric [1–5], solar [6–12], reactor [13], and accelerator neutrinos [14], have demonstrated that neutrinos change flavor as they travel from the source to the detector, a phenomenon consistent with the hypothesis of neutrino oscillation. Neutrino oscillation is a natural consequence of neutrinos that have finite mass and flavor eigenstates that are superpositions of the mass eigenstates. The phenomenon is referred to as oscillation because the survival probability of a given flavor, such as ν_μ, is given by:

$$P(\nu_\mu \to \nu_\mu) = 1 - \sin^2 2\theta \sin^2\left(\frac{1.27\Delta m^2(\mathrm{eV}^2)L(\mathrm{km})}{E(\mathrm{GeV})}\right), \quad (1)$$

where E is the neutrino energy, L is the travel distance, Δm^2 is the difference of the squared mass eigenvalues, and θ is the mixing angle between flavor and mass states. This equation is true in vacuum for all cases, is true in matter for $\nu_\mu \leftrightarrow \nu_\tau$, but may be modified for oscillation involving ν_e which travel through matter.

However, the sinusoidal L/E dependence of the survival probability has not yet been observed. For solar neutrinos, the survival probability is non-sinusoidal as the two eigenstates in matter are no longer coherent after many oscillation cycles [15]. Reactor and accelerator neutrino experiments have insufficient statistics at this time. The standard analysis [1, 16] of the large sample of atmospheric neutrinos recorded by the Super-Kamiokande experiment has not been optimized to resolve the effect, although the zenith angle dependence strongly indicates maximal $\nu_\mu \leftrightarrow \nu_\tau$ mixing with Δm^2 in the vicinity of 2 to 2.5×10^{-3} eV^2. The analysis described herein used a selected sample of these atmospheric neutrino events, those with good resolution in L/E, to search for the dip in oscillation probability expected when the argument of the second sine-squared term in Eq. 1 is $\pi/2$.

Super-Kamiokande (Super-K) is a cylindrical 50 kton water Cherenkov detector located at a depth of 2700 m water equivalent. The water tank is optically separated into two concentric cylindrical detector regions. The inner detector (ID) is instrumented with 11,146 inward facing 20 inch diameter photomultiplier tubes (PMT). The outer detector (OD) is instrumented with 1,885 outward facing 8 inch PMTs.

In the present analysis, 1489 live-day exposure of fully contained (FC) μ-like and partially contained (PC) atmospheric neutrino data were used. FC events deposit all of their Cherenkov light inside the ID, while PC events have an exiting particle that deposits visible energy in the OD. The direction and the momentum of charged particles were reconstructed from the Cherenkov ring image. Each observed ring was identified as either e-like or μ-like based on the shape of the ring pattern. For FC multi-ring events, the particle type of the most energetic ring was used to identify μ-like events. Since more than 97 % of PC events were estimated to be ν_μ charged current (CC) interactions, all PC events were classified as μ-like. The atmospheric neutrino prediction in Super-K is modeled using a Monte Carlo (MC) simulation [16].

Event selection and classification in the present analysis are different from those in the Super-K standard oscillation analysis [1] in two ways. (i) The fiducial volume for the FC sample was expanded from 22.5 kton to 26.4 kton (the event vertex should be more than 1.5 m from the top and bottom walls of the ID and 1 m from the side wall) in order to increase the statistics of the data, especially of high energy muons. Even with the larger fiducial volume, the estimated non-neutrino background was negligibly small, less than 0.1%. (ii) The PC sample was subdivided into two categories: "OD stopping events" where the muon stops in the outer detector, and "OD through-going events" where the muon exits into the rock. The division is based on the amount of Cherenkov light detected in the OD. Figure 1 shows the ratio of the observed number of photoelectrons (p.e.) to the expectation from the projected track length of the muon. Events with smaller number of p.e.'s than the criterion were classified as "OD stopping events". Since these two samples have different resolution in L/E, different cuts were applied for each sample, improving the overall efficiency.

The neutrino energy was estimated from the total energy of charged particles observed in the ID. The energy deposited in the OD was taken into account for PC events. The projected track length in the OD was used to estimate the energy deposited in the OD. The relationship between the neutrino energy and the observed energy was determined based on the MC simulation. The flight length of neutrinos, which ranges from approximately 15 km to 13,000 km depending on the zenith angle, was estimated from the reconstructed neutrino direction. The neutrino direction was taken to be along the total momentum vector from all observed particles. The resolution of the reconstructed L/E was calculated at each point in the $(\cos\Theta, E)$ plane, where Θ is the zenith angle. The energy resolution becomes poorer for higher energy PC events, due mainly to the saturation in the electronics that records the PMT charge. Therefore, extremely high energy events (observed energy > 50 GeV) were excluded in this analysis. All the FC μ-like events

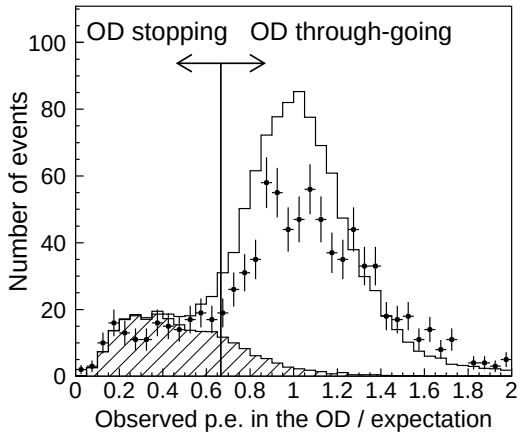

FIG. 1: Observed number of p.e.'s in the OD divided by the expectation from the projected track length of the muon for the data (points), the OD through-going MC events (white region in histogram) and the OD stopping MC events (hatched region). The MC does not include oscillations and is normalized by the live-time. If oscillation is included in the MC, the normalization of the data and MC agrees within 10 %.

		Data	MC	$\nu_\mu + \overline{\nu}_\mu$ CC
FC	single-ring μ-like	1619	2105.8	(98.3 %)
	multi-ring μ-like	502	813.0	(94.2 %)
PC	OD stopping	114	137.0	(95.4 %)
	OD through-going	491	670.4	(99.1 %)

TABLE I: Summary of atmospheric neutrino events used in the present analysis. Only μ-like events are used. Numbers of the MC events are normalized by the live-time. Neutrino oscillation is not included in the MC. Numbers in the parentheses show the estimated fraction of $\nu_\mu + \overline{\nu}_\mu$ CC interactions in each sample.

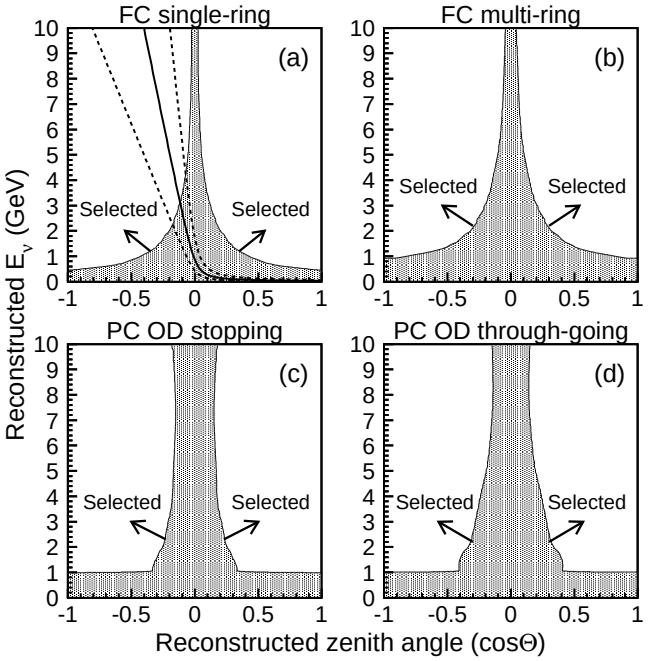

FIG. 2: Contour plots of 70 % L/E resolution in the ($\cos\Theta$, E_ν) plane for (a) FC single-ring, (b) FC multi-ring, (c) PC OD stopping and (d) PC OD through-going samples. Three additional lines in (a) show the survival probabilities of muon neutrinos predicted from neutrino oscillation with $(\sin^2 2\theta,\ \Delta m^2) = (1.00,\ 2.4 \times 10^{-3}\,\mathrm{eV}^2)$. Full and half oscillation occur on the solid and dashed lines, respectively.

have observed energy less than 25 GeV, so this cut is only relevant to PC events. Figure 2 shows 70 % L/E resolution contours, as used for the selection criteria in this analysis. The reasons for the poor L/E resolutions are either large $dL/d\Theta$ for horizontal-going events or large scattering angles for low energy events. The bold solid central line in Fig. 2a indicates the minimum survival probability of muon neutrinos predicted from neutrino oscillations with $\Delta m^2 = 2.4 \times 10^{-3}$ eV^2. It is clear that detecting high energy muon events is crucial to observe the first maximum oscillation in L/E. The resolution cut of $\Delta(L/E) < 70\,\%$ was determined from the MC simulation to maximize the sensitivity to distinguish neutrino oscillation from other hypotheses.

The L/E resolution cut removes 58.8 % of the FC μ-like and 33.6 % of the PC events. Table I summarizes the number of events used in this analysis after the L/E resolution cut. Figure 3 shows the number of events as a function of L/E for the data and MC predictions. Two clusters of events are visible below and above 150 km/GeV. They mostly correspond to downward-going and upward-going events, respectively. Below 150 km/GeV, the data and MC agree well. Above 500 km/GeV, the deficit due to oscillation of upward-going neutrinos is apparent. In Fig. 4 the data over non-oscillated MC ratio as a function of L/E is plotted together with the best-fit expectation for 2-flavor $\nu_\mu \leftrightarrow \nu_\tau$ oscillations with systematic errors. A dip, which should correspond to the first maximum oscillation, is observed around $L/E = 500$ km/GeV. We note that the position of the dip is separated from the event number minimum, the notable feature in Fig. 3. Due to the L/E resolution of the detector, the second and higher maximum oscillation points should not be observable in this experiment.

In order to confirm that the observed dip was not due to systematic effects, several tests were carried out. Several L/E distributions were made by changing the L/E resolution cut value. Plots based on the resolution cuts at 60, 80 and 90% showed consistent dip structures as that based on the 70% cut. Also, L/E plots based on several other L/E bin sizes gave essentially the same results. In addition, the sign of the direction vector for each event was changed artificially. In this artificial data sample, the "upward-going" events should have little disappearance effect and therefore the L/E distribution should not show any dip structure around $L/E = 500$ km/GeV. The

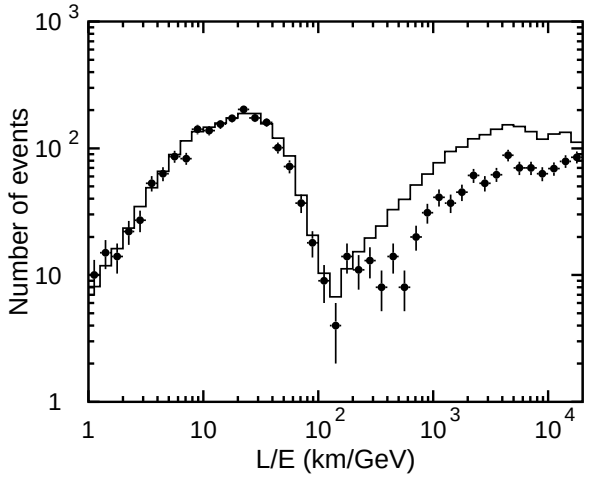

FIG. 3: Number of events as a function of L/E for the data (points) and the atmospheric neutrino MC events without oscillations (histogram). The MC is normalized by the detector live-time.

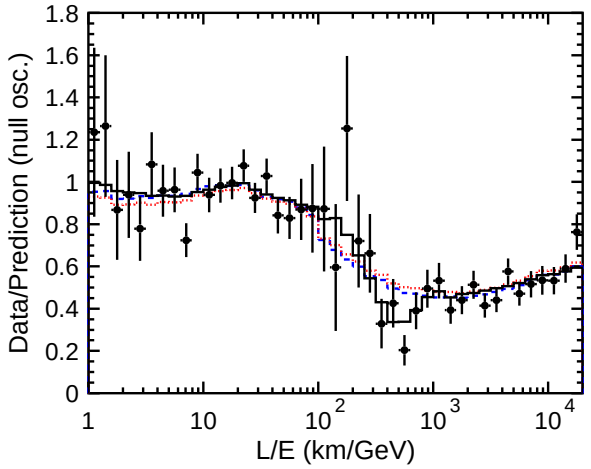

FIG. 4: Ratio of the data to the MC events without neutrino oscillation (points) as a function of the reconstructed L/E together with the best-fit expectation for 2-flavor $\nu_\mu \leftrightarrow \nu_\tau$ oscillations (solid line). The error bars are statistical only. Also shown are the best-fit expectation for neutrino decay (dashed line) and neutrino decoherence (dotted line).

L/E distribution for this artificial data sample did not show any significant dip structure around 500 km/GeV. Finally, the L/E plot was made using FC single-ring e-like events. The e-like distribution was consistent with flat over the whole L/E range. Thus we are confident that the observed dip is not due to systematic effects in the event selection.

The data/prediction at large L/E in Fig. 4 shows a slight rise from the expected flat distribution. We have studied possible causes of this deviation, such as the that an energy-dependent systematic effect, such as the predicted neutrino interaction cross section, are the main sources of the non-flatness. The best-fit L/E distribution for oscillations, allowing systematic terms to vary within the estimated uncertainty (as described below), also shows this rise with respect to no-oscillation prediction, as seen in the curves overlaid in Fig. 4. The rise at large L/E is consistent with the data.

The observed L/E distribution was fit assuming $\nu_\mu \leftrightarrow \nu_\tau$ oscillations. The L/E distribution was divided into 43 bins from $log(L/E) = 0.0$ to 4.3. The likelihood of the fit and the χ^2 were defined as:

$$\mathcal{L}(N^{\rm prd}, N^{\rm obs}) = \prod_{i=1}^{43} \frac{\exp(-N_i^{\rm prd})(N_i^{\rm prd})^{N_i^{\rm obs}}}{N_i^{\rm obs}!} \times \prod_{j=1}^{24} \exp\left(-\frac{\epsilon_j^2}{2\sigma_j^2}\right), \quad (2)$$

$$N_i^{\rm prd} = N_i^0 \cdot P(\nu_\mu \to \nu_\mu) \cdot (1 + \sum_{j=1}^{25} f_j^i \cdot \epsilon_j), \quad (3)$$

$$\chi^2 \equiv -2 \ln \left(\frac{\mathcal{L}(N^{\rm prd}, N^{\rm obs})}{\mathcal{L}(N^{\rm obs}, N^{\rm obs})} \right), \quad (4)$$

where $N_i^{\rm obs}$ is the number of the observed events in the i-th bin and $N_i^{\rm prd}$ is the number of predicted events, in which neutrino oscillation and systematic uncertainties are considered. N_i^0 is the MC predicted number of events without oscillation for the i-th bin. Various systematic uncertainties are represented by 25 parameters ϵ_j, which include 7 uncertainty parameters from the flux calculation, 3 from the detector calibration and background, 2 from the data reduction, 5 from the event reconstruction, and 8 from the neutrino interaction simulation. Among these, only 24 constrain the likelihood as the absolute normalization is allowed to be free. A more detailed description of the systematic error terms can be found in Ref. [16]. The second term in the likelihood definition represents the contributions from the systematic errors, where σ_j is the estimated uncertainty in the parameter ϵ_j. The fractional effect of systematic error term ϵ_j on the i-th bin is given by f_j^i.

A scan was carried out on a $(\sin^2 2\theta, \log \Delta m^2)$ grid, minimizing χ^2 by optimizing the systematic error parameters at each point. The minimum χ^2 was 37.9/40 DOF at $(\sin^2 2\theta, \Delta m^2) = (1.00, 2.4\times10^{-3}\,{\rm eV}^2)$. Including the unphysical region ($\sin^2 2\theta > 1$), the best-fit was obtained at $(\sin^2 2\theta, \Delta m^2) = (1.02, 2.4 \times 10^{-3}\,{\rm eV}^2)$, in which the minimum χ^2 was 0.12 lower than that in the physical region. Figure 5 shows the contour plot of the allowed oscillation parameter regions. Three contours correspond to the 68 %, 90 % and 99 % confidence level (C.L.) allowed regions, which are defined to be $\chi^2 = \chi^2_{min} +$ 2.48, 4.83, and 9.43, respectively, where χ^2_{min} is the minimum χ^2 in the physical region. These intervals are derived based on the extension of the method described in

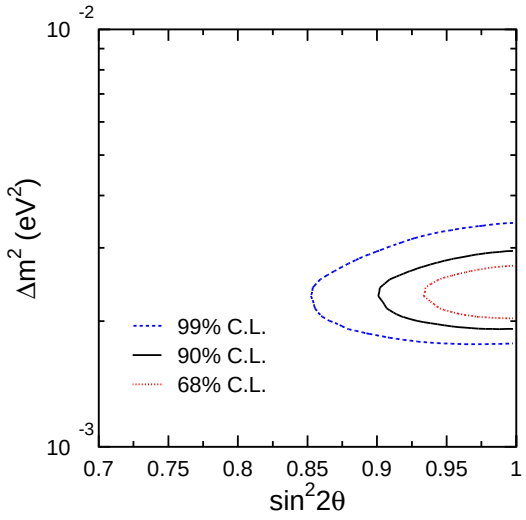

FIG. 5: 68, 90 and 99% C.L. allowed oscillation parameter regions for 2-flavor $\nu_\mu \leftrightarrow \nu_\tau$ oscillations obtained by the present analysis.

Ref. [17]. The 90 % C.L. allowed parameter region was obtained as $1.9 \times 10^{-3}\,\mathrm{eV}^2 < \Delta m^2 < 3.0 \times 10^{-3}\,\mathrm{eV}^2$ and $\sin^2 2\theta > 0.90$. The location of the allowed region is consistent with that of the oscillation analysis using zenith angle distributions [1, 16].

In order to evaluate the significance of the dip in L/E, a null hypothesis that accounts for the basic shape due to the disappearance of neutrinos is needed. The no-oscillation case is not useful as it is very strongly disfavored by the data at large L/E ($\chi^2_{no\,osc} = 212.7/42\,\mathrm{DOF}$). We used two alternative hypotheses that basically reproduce the zenith angle dependent deficit, predicting that about half of the muon neutrinos smoothly disappear at large L/E. These hypotheses are neutrino decay [18, 19] and neutrino decoherence [20, 21]. The ν_μ survival probability for neutrino decay is expressed as $P(\nu_\mu \to \nu_\mu) = \left[\sin^2\theta + \cos^2\theta \exp\left(-m/2\tau \cdot L/E\right)\right]^2$ where θ is the mixing angle and τ is the lifetime of a neutrino mass state. The neutrino decoherence survival probability is $P(\nu_\mu \to \nu_\mu) = 1 - \frac{1}{2}\sin^2 2\theta\,[1 - \exp\left(-\gamma_0 L/E\right)]$, where θ is the mixing angle and γ_0 is the decoherence parameter. Figure 4 includes the L/E distribution for the best-fit expectation for neutrino decay and decoherence. The ${\chi^2}_{min}$ values were 49.1/40 DOF at ($\cos^2\theta$, m/τ) = (0.33, 1.26×10^{-2} GeV/km) for neutrino decay and 52.4/40 DOF at ($\sin^2 2\theta$, γ_0) = (1.00, 1.23×10^{-21} GeV/km) for neutrino decoherence. These χ^2_{min} values were 11.3 (3.4 standard deviations) and 14.5 (3.8 standard deviations) larger than χ^2_{min} for neutrino oscillation.

In order to check the statistical significance against the alternative models, 10,000 MC L/E distributions were produced assuming neutrino decay with the best fit decay parameters. Each L/E distribution was fitted assuming neutrino decay and oscillation, and the χ^2 difference for these two assumptions was calculated. Only 11 among 10,000 samples had χ^2 for neutrino decay smaller by 11.3 or more than the same sample evaluated for neutrino oscillation. Therefore, the probability that neutrino decay could mimic neutrino oscillations is approximately 0.1% as naively expected by 3.4 standard deviations. The neutrino decoherence model is disfavored more strongly.

In summary, we have studied the survival probability of muon neutrinos as a function of L/E using atmospheric neutrino events observed in Super-Kamiokande. A dip in the L/E distribution was observed around L/E = 500 km/GeV. This strongly constrains Δm^2. Alternative models that could explain the zenith angle and energy dependent deficit of the atmospheric muon neutrinos are disfavored, since they do not predict any dip in the L/E distribution. We conclude that the observed L/E distribution gives the first direct evidence that the neutrino survival probability obeys the sinusoidal function as predicted by neutrino flavor oscillations.

We gratefully acknowledge the cooperation of the Kamioka Mining and Smelting Company. The Super-Kamiokande experiment has been built and operated from funding by the Japanese Ministry of Education, Culture, Sports, Science and Technology, the United States Department of Energy, and the U.S. National Science Foundation.

* Present address: Enrico Fermi Institute, University of Chicago, Chicago, IL 60637, USA

[1] Y. Fukuda et al., Phys. Rev. Lett. **81**, 1562 (1998).
[2] Y. Fukuda et al., Phys. Lett. **B335**, 237 (1994).
[3] R. Becker-Szendy et al., Phys. Rev. **D46**, 3720 (1992).
[4] M. Ambrosio et al., Phys. Lett. **B434**, 451 (1998).
[5] M. Sanchez et al., Phys. Rev. **D68**, 113004 (2003).
[6] B. T. Cleveland et al., Astrophys. J. **496**, 505 (1998).
[7] Y. Fukuda et al., Phys. Rev. Lett. **77**, 1683 (1996).
[8] W. Hampel et al., Phys. Lett. **B447**, 127 (1999).
[9] J. N. Abdurashitov et al., J. Exp. Theor. Phys. **95**, 181 (2002).
[10] M. Altmann et al., Phys. Lett. **B490**, 16 (2000).
[11] M. B. Smy et al., Phys. Rev. **D69**, 011104 (2004).
[12] S. N. Ahmed et al. (2003), nucl-ex/0309004.
[13] K. Eguchi et al., Phys. Rev. Lett. **90**, 021802 (2003).
[14] M. H. Ahn et al., Phys. Rev. Lett. **90**, 041801 (2003).
[15] P. C. de Holanda and A. Y. Smirnov (2003), hep-ph/0309299.
[16] Y. Ashie et al. (Super-Kamiokande) (2004), draft in preparation.
[17] R. M. Barnett et al. (Particle Data Group), Phys. Rev. **D54**, 1 (1996).
[18] V. Barger, J. G. Learned, S. Pakvasa, and T. J. Weiler, Phys. Rev. Lett. **82**, 2640 (1999).
[19] V. Barger et al., Phys. Lett. **B462**, 109 (1999).
[20] Y. Grossman and M. P. Worah (1998), hep-ph/9807511.
[21] E. Lisi, A. Marrone, and D. Montanino, Phys. Rev. Lett. **85**, 1166 (2000).